Solar Physics (2006) 233: 185–204
DOI: 10.1007/s11207-006-1636-6

THE ALPHA EFFECT AND THE OBSERVED TWIST AND CURRENT HELICITY OF SOLAR MAGNETIC FIELDS

K. M. KUZANYAN
National Astronomical Observatories, Chinese Academy of Sciences, Beijing, China; Institute for Terrestrial Magnetism, Ionosphere and Radiowave Propagation (IZMIRAN), Troitsk, Moscow Region, Russia; Department of Applied Mathematics, University of Leeds, Leeds, U.K.
(e-mail: kuzanyan@maths.leeds.ac.uk)

V. V. PIPIN
Institute for Solar-Terrestrial Physics, Irkutsk, Russia
(e-mail: pip@iszf.irk.ru)

and

N. SEEHAFER
Institut für Physik, Universität Potsdam, Germany
(e-mail: seehafer@agnld.uni-potsdam.de)

(Received 19 May 2003; accepted 28 October 2005)

Abstract. We present a straightforward comparison of model calculations for the α-effect, helicities, and magnetic field line twist in the solar convection zone with magnetic field observations at atmospheric levels. The model calculations are carried out in a mixing-length approximation for the turbulence with a profile of the solar internal rotation rate obtained from helioseismic inversions. The magnetic field data consist of photospheric vector magnetograms of 422 active regions for which spatially-averaged values of the force-free twist parameter and of the current helicity density are calculated, which are then used to determine latitudinal profiles of these quantities. The comparison of the model calculations with the observations suggests that the observed twist and helicity are generated in the bulk of the convection zone, rather than in a layer close to the bottom. This supports two-layer dynamo models where the large-scale toroidal field is generated by differential rotation in a thin layer at the bottom while the α-effect is operating in the bulk of the convection zone. Our previous observational finding was that the moduli of the twist factor and of the current helicity density increase rather steeply from zero at the equator towards higher latitudes and attain a certain saturation at about $12 - 15^\circ$. In our dynamo model with algebraic nonlinearity, the increase continues, however, to higher latitudes and is more gradual. This could be due to the neglect of the coupling between small-scale and large-scale current and magnetic helicities and of the latitudinal drift of the activity belts in the model.

1. Introduction

The α-effect is generally considered as the central mechanism of a mean-field dynamo (Moffatt, 1978; Parker, 1979; Krause and Rädler, 1980; Zeldovich, Ruzmaikin, and Sokoloff, 1983; Roberts and Soward, 1992; Ossendrijver, 2003; Rüdiger and Arlt, 2003). In astrophysical bodies this effect, along with differential

rotation, provides for the generation of magnetic fields from turbulent convective motions under the influence of rotation. While for the solar convection zone rather reliable and detailed information on the variation of the rotation rate with radius and latitude can be obtained using helioseismic inversions of solar oscillations measurements (*e.g.*, Schou *et al.*, 1998), there is presently no comparable method to probe the α-effect. Also, detailed theoretical predictions concerning the α-effect in the solar convection zone are still missing.

The α-effect corresponds to a mean electromotive force (emf), $\mathcal{E} = \alpha\langle\mathbf{B}\rangle$ proportional to the mean magnetic field $\langle\mathbf{B}\rangle$ (angular brackets denote averages) due to fluctuations of the velocity and magnetic field; the coefficient α occurring here is in general a tensorial quantity. This effect was introduced by Steenbeck, Krause, and Rädler (1966) as a mechanism linked to the mean kinetic helicity density of turbulent fluid motions. The densities (per unit volume) of kinetic, magnetic, and current helicity are defined by

$$h_{\mathrm{k}} = \mathbf{v}\cdot(\nabla\times\mathbf{v}), \quad h_{\mathrm{m}} = \mathbf{A}\cdot(\nabla\times\mathbf{A}), \quad h_{\mathrm{c}} = \mathbf{B}\cdot(\nabla\times\mathbf{B}), \tag{1}$$

where $\mathbf{v}$ is the fluid velocity and $\mathbf{A}$ a magnetic vector potential; h_{m} and h_{c} are closely related. For isotropic situations, where α is a scalar, traditionally the estimate

$$\alpha \approx -\frac{\tau_{\mathrm{cor}}}{3}\langle\mathbf{u}\cdot(\nabla\times\mathbf{u})\rangle \tag{2}$$

is used (Steenbeck, Krause, and Rädler, 1966; Krause and Rädler, 1980), where τ_{cor} is the correlation time of the velocity fluctuations $\mathbf{u}$. Relations between the α-effect and magnetic as well as current helicity were noticed by Frisch *et al.* (1975) and Pouquet, Frisch, and Léorat (1976); see also Moffatt (1978), Kleeorin and Ruzmaikin (1982) and Zeldovich, Ruzmaikin, and Sokoloff (1983). More recently it was found that the α-effect is connected with the current helicity of the fluctuations by a relation of the form

$$\sum_{i,j}\alpha_{ij}\langle B_i\rangle\langle B_j\rangle = -\eta\langle\mathbf{b}\cdot(\nabla\times\mathbf{b})\rangle \tag{3}$$

(Keinigs, 1983; Matthaeus, Goldstein, and Lantz, 1986; Rädler and Seehafer, 1990; Seehafer, 1994, 1996), valid if the magnetic fluctuations $\mathbf{b}$ are statistically homogeneous in space and time; η is the magnetic diffusivity. In the isotropic case, α is then a scalar given by

$$\alpha = -\frac{\eta}{\langle\mathbf{B}\rangle^2}\langle\mathbf{b}\cdot(\nabla\times\mathbf{b})\rangle\,, \tag{4}$$

while Equation (3) reduces to the approximate relation

$$\alpha_{\varphi\varphi}\langle B_\varphi\rangle^2 \approx -\eta\langle\mathbf{b}\cdot(\nabla\times\mathbf{b})\rangle, \tag{5}$$

if the toroidal component $\langle B_\varphi\rangle$ of the mean magnetic field is large compared to the other components, as is presumably the case for the Sun.

Both the kinetic (Rüdiger, Brandenburg, and Pipin, 1999; Duvall and Gizon, 2000) and current helicities are observable at the surface of the Sun. In this paper we use data deduced for the current helicity. The observational material available for the kinetic helicity is too sparse at present. Current helicity can be determined on the basis of magnetic field measurements both in the atmosphere (Seehafer, 1990; Rust and Kumar, 1994; Pevtsov, Canfield, and Metcalf, 1995; Abramenko, Wang, and Yurchishin, 1996; Bao and Zhang, 1998; Zhang and Bao, 1998; López Fuentes *et al.*, 2003; Hagino and Sakurai, 2004) and in interplanetary plasma clouds ejected from the Sun (Rust, 1994; Bothmer and Schwenn, 1998; Dasso *et al.*, 2003; Ruzmaikin, Martin, and Hu, 2003; Leamon, Canfield, and Pevtsov, 2004). In addition, there are indirect indicators of current helicity, for instance chirality patterns in and around sunspots (Hale, 1927; Richardson, 1941; Ding, Hong, and Wang, 1987) or filaments (Martin, Bilimoria, and Tracadas, 1994) as well as sigmoids, *i.e.*, S or reverse-S-shaped brightenings (Rust and Kumar, 1996; Canfield, Hudson, and McKenzie, 1999; Pevtsov, 2002); see also reviews by Zirker *etal.* (1997), Martin (1998), Rust (2001) and Low (2001).

At superphotospheric levels the magnetic force dominates over all other forces, except for times of explosive events. Therefore the magnetic field is approximately force-free there in general, satisfying

$$\nabla \times \mathbf{B} = \alpha_{\mathrm{ff}} \mathbf{B}, \quad \alpha_{\mathrm{ff}} = \frac{h_{\mathrm{c}}}{\mathbf{B}^2}, \tag{6}$$

where α_{ff} is a (pseudo) scalar that is constant along magnetic field lines. From the observations it is found that α_{ff} and h_{c} are predominantly negative in the northern and positive in the southern hemisphere of the Sun. If the parameter α_{ff} of the force-free field is spatially constant, h_{m} and h_{c} have the same sign (*cf.* Seehafer, 1990). This can be expected to be still approximately valid if α_{ff} has a predominant sign within individual active regions, as indicated by the observations. Thus, the magnetic helicity density h_{m} is presumably also predominantly negative in the northern and positive in the southern hemisphere.

The α-effect corresponds to the simultaneous generation of magnetic helicities in the mean field and in the fluctuations, the generation rates being equal in magnitude and opposite in sign (Seehafer, 1996). The mean total magnetic helicity, which is an invariant of ideal magnetohydrodynamics, is not influenced by the α-effect. The two magnetic helicities generated by the α-effect, that in the mean field and that in the fluctuations, have either to be dissipated *in situ* or to be transported out of the generation region. The latter can explain the observed appearance of magnetic helicity in the solar atmosphere and in interplanetary space. A similar segregation of magnetic helicities with opposite sign occurs in a scenario termed the Σ-effect (Longcope, Fisher, and Pevtsov, 1998; Longcope *et al.*, 1999; Longcope and Pevtsov, 2003). Here the action of a helical turbulent velocity field on isolated magnetic flux tubes generates twist of one sign which is compensated by a generation of writhe (helical deformation of the tube axis) with the opposite sign.

This process is assumed to operate during the rise of the flux tubes through the convection zone.

Besides the α-effect (or the Σ-effect), the Ω-effect (that is, differential rotation) may also generate magnetic helicity in the convection zone (Berger and Ruzmaikin, 2000). In a number of studies the generation of magnetic helicity by the differential rotation of the photospheric footpoints of coronal magnetic structures was considered (Raadu, 1972; van Ballegooijen and Martens, 1990; van Ballegooijen, Cartledge, and Priest, 1998; DeVore, 2000; Démoulin *et al.*, 2002). In the model calculation presented in this paper the generation of small-scale helicity due to the shear action of the differential rotation in the convection zone is included.

The close connection between current helicity and α-effect on the one hand and the present level of observational resolution on the basis of systematic studies of magnetic fields and their current helicity on the other hand provide an opportunity to gain insight into the dynamo operation in the convection zone and, in particular, the role of the α-effect. The objective of this paper is to develop theoretical models for the α-effect and to adjust them to its available observational tracers.

The natural sources of helicity and the α-effect in cosmical bodies are the action of Coriolis forces on turbulent fluid motions and a stratification of the mean mass density and/or turbulence intensity (Moffatt, 1978; Krause and Rädler, 1980; Rüdiger and Kichatinov, 1993). The Coriolis forces may be due to rigid or differential rotation. Hitherto in most calculations of the α-effect, rigid rotation has been assumed. However, a gradient of the rotation rate, or velocity shear, may significantly influence the turbulence in a small layer near the base of the solar convective zone and thus the turbulent electromotive force. This has to be distinguished from the direct effect of differential rotation on the large scale, *i.e.*, the generation of a mean toroidal field from a mean poloidal one.

We calculate the α-effect in the framework of mean-field magnetohydrodynamics using a realistic profile $\Omega(r, \theta)$ of the solar internal rotation rate as a function of radius r and co-latitude θ obtained by means of helioseismic inversions by Schou *et al.* (1998). Radial profiles of other quantities needed are derived from a standard model of the solar interior (Stix, 2002). In this way, in particular, the important effects of both the mean density stratification and of the stratification of the turbulence intensity in the convection zone are included into the calculations. The turbulent velocity fluctuations are assumed to be driven by (i) a prescribed random body force resulting from thermal convection and (ii) the Lorentz force due to prescribed magnetic background fluctuations. The two driving forces give rise to two contributions to the α-effect, termed the hydrodynamic and the magnetic part of the α-effect. Helicity develops in a natural way if the driven background velocity fluctuations, as present in the absence of rotation and a mean magnetic field, are acted upon by Coriolis forces and velocity shear.

In this study we extend work by Rüdiger and Kichatinov (1993), Rüdiger and Pipin (2000), Rüdiger, Pipin, and Belvedere (2001), and Pipin (2003). We also extend and partially correct results from a preceding step of our investigations

(Seehafer *et al.*, 2003) where (i) only the magnetic part of the α-effect was calculated and, more important, (ii) stratification effects were not taken into account – helicity generation and α-effect were due to compressibility effects instead (*i.e.*, density fluctuations and buoyancy effects connected with them), which turned out, however, to be in general (*i.e.*, except for the near-surface layers of the convection zone) much weaker than the stratification effects that are included in the present study. Therefore, (i) the conclusion concerning the region in the convection zone where the α-effect works was different and (ii) the strength of the α-effect and the helicity generation rate were about an order of magnitude smaller in the preceding study compared to the present one. For a model of the evolution of magnetic helicity over a solar activity cycle, over which we average in the present study, we refer to Kleeorin *et al.* (2003).

The plan of the paper is as follows. In Section 2 we review magnetic field observations relevant for our study, followed by the presentation of the theoretical calculations in Section 3. Then, in Section 4, we estimate some important model parameters and compare them with observations. In Section 5, finally, we discuss our results.

2. Review of the Analysis of Observational Tracers of the α-Effect

Recently in a number of papers, systematic studies of magnetographic observations in solar active regions were reported aiming at identifying observational tracers of the α-effect. We here briefly describe the results of Kuzanyan, Bao, and Zhang (2000) and Zhang, Bao, and Kuzanyan (2002).

The coefficient $\alpha_{\rm ff}$ of the force-free magnetic field, defined by the first part of Equation (6), is a very useful quantity for studying the atmospheric fields. It is a simple function of the field-line geometry (*cf.* Boström, 1973) and can be interpreted as the torsion of neighbouring field lines about each other or field line twist. Kuzanyan, Bao, and Zhang (2000) and Zhang, Bao, and Kuzanyan (2002) calculated both a mean force-free coefficient

$$\langle \alpha_{\rm ff} \rangle \approx \left\langle \frac{(\nabla \times \mathbf{B})_\parallel}{\mathbf{B}_\parallel} \right\rangle \tag{7}$$

and a mean current helicity density

$$\langle h_{\rm c} \rangle \approx \langle \mathbf{B}_\parallel \cdot (\nabla \times \mathbf{B})_\parallel \rangle \tag{8}$$

(the index $_\parallel$ denotes longitudinal, *i.e.*, line-of-sight components of vectors). In Equation (8) the contribution of the transverse component of the electric current is neglected, as it cannot be determined from magnetographic observations at a single photospheric level. The dataset used consists of 422 photospheric vector magnetograms of active regions obtained with the vector magnetograph at the Huairou Solar Observing Station in the period 1988 – 1997. It includes most of the

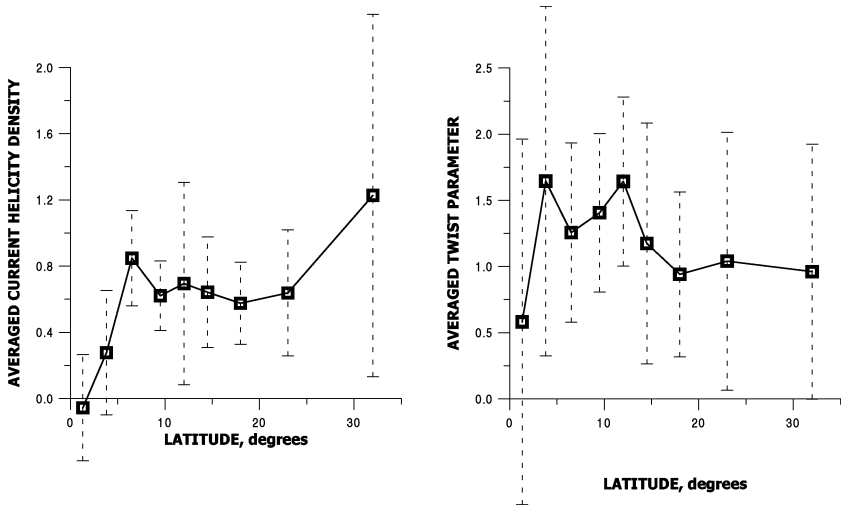

Figure 1. Observed absolute values of the mean current helicity, $|\langle h_c \rangle| = |\langle \mathbf{B}_\parallel \cdot (\nabla \times \mathbf{B})_\parallel \rangle|$ (*left panel*) and the mean twist parameters $|\langle \alpha_{ff} \rangle|$ (*right panel*) versus absolute latitude in degrees. The variable h_c is measured in $10^{-3}\, G^2\, m^{-1}$ and α_{ff} in $10^{-8}\, m^{-1}$. Averages were taken over nine latitude intervals between the equator, 2.5°, 5°, 8°, 11°, 13°, 16°, 20°, 26°, 38° in each hemisphere. Vertical lines show 95% confidence intervals. The latitudinal intervals were chosen such as to have approximately equal numbers of observational points in each interval, and thus a high level of confidence.

large active regions in this time period. $\langle \alpha_{ff} \rangle$ and $\langle h_c \rangle$ were computed as in Bao and Zhang (1998), that is, mean values were obtained by averaging over spatial scales of the order of 5° in solar latitude, which is a scale slightly smaller than the size of active regions, and times of the order of one Carrington rotation, *i.e.*, 27 days.

In Figure 1 the moduli of the two tracers of the α-effect show a steep increase from zero at the equator towards higher latitudes. This steep increase ends at about 12 – 15° where a kind of first local maximum or plateau is probably attained and the variation with latitude becomes more gradual. This observation was reported earlier in Seehafer *et al.* (2003). We wish to note here that, since the data are very noisy, the existence of the plateau needs to be confirmed by the analysis of additional observational material in the future.

Latitudinal distributions of the force-free factor and the current helicity were also presented in previous studies using other data sets, *e.g.*, Longcope, Fisher, and Pevtsov (1998), Pevtsov and Canfield (1999), Pevtsov and Latushko (2000), and Pevtsov, Canfield, and Latushko (2001). In these studies latitudinal distributions were determined both for the magnetic fields of active regions and for the large-scale solar magnetic field, but latitudinal profiles as presented in this paper for the active-region fields, obtained by taking averages over appropriate latitudinal intervals, seem to have been computed only for the large-scale field. The computations for the large-scale field were based on time series of line-of-sight full-disk magnetograms. Pevtsov and Latushko (2000) calculated latitudinal profiles of the current-helicity

density using two different data sets. The hemispheric sign rule – negative helicity in the north and positive helicity in the south – is confirmed only for higher latitudes ouside of the active-region belts. On the other hand, our data are restricted to latitudes below $\pm 30^\circ$. For these low latitudes, the helicity of the large-scale field computed by Pevtsov and Latushko (2000) shows strong noise and sign reversals. At least for one of their two data sets, the calculated helicity at low latitudes is clearly positive in the North and negative in the South. This confirms the expectation (see Section 1) that the magnetic helicity of the large-scale field should be opposite in sign to that of the small-scale field (which presumably appears in the form of active regions). Moreover, the modulus of the calculated helicity of the large-scale field increases from the equator towards higher latitudes to reach a local maximum at about 15°. Altogether this seems to be in reasonable agreement with the observation that the moduli of $\langle \alpha_{\rm ff} \rangle$ and $\langle h_{\rm c} \rangle$ increase steeply from zero at the equator to reach some kind of plateau at about $12 - 15^\circ$.

3. Theoretical Calculation of $\alpha_{\varphi\varphi}$, $\langle h_{\rm c} \rangle$ and $\langle h_{\rm k} \rangle$

3.1. General formalism

In our theoretical derivations we use a co-rotating frame of reference and assume the existence of a background turbulence that is independent of the mean flow (*i.e.*, the differential rotation) and the mean magnetic field. The magnetic field is decomposed into mean and fluctuating parts according to

$$B_i = \langle B_i \rangle + b_i , \tag{9}$$

and the equation for the fluctuating part **b** reads

$$\frac{\partial \mathbf{b}}{\partial t} = \nabla \times (\mathbf{u} \times \langle \mathbf{B} \rangle + \mathbf{V} \times \mathbf{b} + \varepsilon) + \eta \nabla^2 \mathbf{b} + \mathfrak{G} , \tag{10}$$

where **u** denotes the fluctuating velocity and **V** the velocity of the differential rotation, ε is a fluctuating electric field driving the magnetic background fluctuations and $\mathfrak{G}$ stands for the nonlinear contributions of the fluctuating fields **u** and **b**. Neglecting fluctuations of the mean mass density (ρ) and taking the density stratification scale vector ($\mathbf{G} = \nabla \log(\rho)$) as well as the mean magnetic field ($\langle \mathbf{B} \rangle$) as constant vectors, we get for the fluctuating momentum density, $\mathbf{m} = \rho \mathbf{u}$

$$\begin{aligned} \frac{\partial m_i}{\partial t} + 2\,(\mathbf{\Omega} \times \mathbf{m})_i = {} & \frac{(\langle \mathbf{B} \rangle \cdot \nabla)\, b_i}{\mu_0} - \nabla_j (V_i m_j + V_j m_i) \\ & - \nabla_i \left(p + \frac{(\langle \mathbf{B} \rangle \cdot \mathbf{b})}{\mu_0} - \nu \frac{(\mathbf{G} \cdot \mathbf{m})}{3} \right) \\ & + \nu (\nabla^2 m_i - (\mathbf{G} \cdot \nabla)\, m_i) + f_i + \mathfrak{F}_i , \end{aligned} \tag{11}$$

where $\mathbf{\Omega}$ is the angular velocity of the solar rotation, p the fluctuating pressure, ν the kinematic viscosity, $\mathbf{f}$ a random body force describing the effects of thermal buoyancy (*cf.* Kichatinov and Rüdiger, 1992; Rüdiger and Kichatinov, 1993) and $\mathfrak{F}$ stands for the nonlinear contributions of the fluctuating fields.

Decomposing into Fourier modes, $\sim \exp\{i(\mathbf{z}\cdot\mathbf{x} - \omega t)\}$ with wave vector $\mathbf{z}$ and frequency ω, Equations (10) and (11) are transformed into equations for the spectrum amplitudes (indicated by circumflexes) of the fluctuating fields:

$$\Delta_\eta \hat{b}_i = \imath\,(\langle\mathbf{B}\rangle\cdot\mathbf{z}) + \frac{(\langle\mathbf{B}\rangle\cdot\mathbf{z})}{\rho} G_n \frac{\partial \hat{m}_i}{\partial z_n} + \langle B_i\rangle \frac{(\mathbf{G}\cdot\hat{\mathbf{m}})}{\rho} + V_{in}\hat{b}_n + V_{ln} z_l \frac{\partial \hat{b}_i}{\partial z_n} + \imath\,(\mathbf{z}\times\hat{\varepsilon})_i + \hat{\mathfrak{G}}_i\,, \tag{12}$$

$$(\Delta_\nu + \imath\nu\,(\mathbf{G}\mathbf{z}))\,\hat{m}_i = -2\frac{(\Omega\mathbf{z})}{\mathbf{z}^2}\,(\mathbf{z}\times\hat{\mathbf{m}})_i + \imath\frac{(\mathbf{z}\cdot\langle\mathbf{B}\rangle)}{\mu_0}\hat{b}_i - \pi_{in}V_{nl}\hat{m}_l + \pi_{if}V_{ln}z_l\frac{\partial \hat{m}_f}{\partial z_n} + \hat{f}_i^{(\mathrm{s})} + \hat{\mathfrak{F}}_i^{(\mathrm{s})}\,, \tag{13}$$

where the equation of mass conservation, $\nabla\cdot\mathbf{m} = 0$, has been employed and the abbreviations, $\Delta_\eta = \eta z^2 - i\omega$ and $\Delta_\nu = \nu z^2 - i\omega$, are used; V_{ij} is the velocity gradient tensor (*i.e.*, $V_{ij} = \partial V_i/\partial r_j$, with $\mathbf{r}$ denoting the position vector), which is taken as homogeneous, $\pi_{ij} = \pi_{ij}(\mathbf{z}) = \delta_{ij} - z_i z_j/z^2$ is the solenoidal projection tensor and $\hat{f}_i^{(\mathrm{s})} = \pi_{ij}\hat{f}_j$ and $\hat{\mathfrak{F}}_i^{(\mathrm{s})} = \pi_{ij}\hat{\mathfrak{F}}_j$ are the solenoidal parts of $\hat{f}_i$ and $\hat{\mathfrak{F}}_i$, respectively (in the following the index $^{(\mathrm{s})}$ always denotes the solenoidal part of a vector). The random force ($\mathbf{f}$) and the random electric field (ε) can be expressed by the background turbulence as driven in the absence of rotation and mean magnetic field by using the relations

$$\Delta_\eta \hat{b}_i^{(0)} = \imath\,(\mathbf{z}\times\hat{\varepsilon})_i + \hat{\mathfrak{G}}_i^{(0)}, \tag{14}$$

$$(\Delta_\nu + \imath\nu\,(\mathbf{G}\cdot\mathbf{z}))\,\hat{m}_i^{(0)} = \hat{f}_i^{(\mathrm{s})} + \hat{\mathfrak{F}}_i^{(\mathrm{s},0)}, \tag{15}$$

obtained from Equations (12) and (13); the index $^{(0)}$ refers to the background turbulence. In the sense of the mixing-length approximation, the sums of time derivatives and nonlinear terms are replaced by τ-relaxation terms with the relaxation time τ given by the correlation time τ_{cor} of the turbulence (Durney and Spruit, 1979), *i.e.*, $-\imath\omega\hat{\mathbf{b}} - \hat{\mathfrak{G}} = \hat{\mathbf{b}}/\tau_{\mathrm{cor}}$, $-\imath\omega\hat{\mathbf{m}} - \hat{\mathfrak{F}}^{(\mathrm{s})} = \hat{\mathbf{m}}/\tau_{\mathrm{cor}}$. In addition, assuming the kinetic and magnetic Reynolds numbers to be high, the diffusive terms proportional to ν or η are neglected. The resulting system of equations reads

$$\hat{b}_i = \hat{b}_i^{(0)} + \imath\tau_{\mathrm{cor}}\,(\langle\mathbf{B}\rangle\cdot\mathbf{z}) + \tau_{\mathrm{cor}}\frac{(\langle\mathbf{B}\rangle\cdot\mathbf{z})}{\rho}G_n\frac{\partial\hat{m}_i}{\partial z_n} + \tau_{\mathrm{cor}}\langle B_i\rangle\frac{(\mathbf{G}\cdot\hat{\mathbf{m}})}{\rho} + \tau_{\mathrm{cor}}V_{in}\hat{b}_n + \tau_{\mathrm{cor}}V_{ln}z_l\frac{\partial\hat{b}_i}{\partial z_n}\,, \tag{16}$$

$$\hat{m}_i = \hat{m}_i^{(0)} - 2\tau_{\rm cor}\frac{(\boldsymbol{\Omega}\cdot\mathbf{z})}{\mathbf{z}^2}(\mathbf{z}\times\hat{\mathbf{m}})_i + \imath\,\tau_{\rm cor}\frac{(\mathbf{z}\cdot\langle\mathbf{B}\rangle)}{\mu_0}\hat{b}_i$$
$$- \tau_{\rm cor}\pi_{in}V_{nl}\hat{m}_l + \tau_{\rm cor}\pi_{if}V_{ln}z_l\frac{\partial\hat{m}_f}{\partial z_n}\,. \tag{17}$$

The system of Equations (16) and (17) can be solved using a perturbation procedure for small values of $\mathbf{G}$ and V_{ij}.

The background turbulence is assumed to be stationary and quasi-isotropic as modeled by Kichatinov (1987) (see also Kichatinov, 1991; Kichatinov and Rüdiger, 1992; Rüdiger and Kichatinov, 1993):

$$\left\langle\hat{m}_i^{(0)}(\mathbf{z},\omega)\hat{m}_j^{(0)}(\mathbf{z}',\omega')\right\rangle = \frac{\hat{E}\,(k,\omega,\kappa)}{16\pi k^2}\delta(\omega+\omega')$$
$$\times\left(\pi_{ij}(\mathbf{k}) + \frac{1}{2k^2}(\kappa_i k_j - \kappa_j k_i)\right), \tag{18}$$

where $\mathbf{k} = \left(\mathbf{z}-\mathbf{z}'\right)/2$, $\boldsymbol{\kappa} = \mathbf{z}+\mathbf{z}'$ and the function $\hat{E}(k,\omega,\kappa)$ is the Fourier transform of the local energy spectrum function ($E(k,\omega,\mathbf{r})$), with the wave vector ($\boldsymbol{\kappa}$) describing a large-scale inhomogeneity of the background turbulence. The relations

$$\left\langle m^{(0)\,2}\right\rangle = \int E\,(k,\omega,\mathbf{r})\,\mathrm{d}k\,\mathrm{d}\omega\,,\quad E\,(k,\omega,\mathbf{r}) = \int \hat{E}(k,\omega,\kappa)e^{i\boldsymbol{\kappa}\cdot\mathbf{r}}\mathrm{d}^3\boldsymbol{\kappa},$$
$$\left\langle u^{(0)\,2}\right\rangle = \int q\,(k,\omega,\mathbf{r})\,\mathrm{d}k\,\mathrm{d}\omega\,,\quad E\,(k,\omega,\mathbf{r}) = \rho^2\,(\mathbf{r})\,q(k,\omega,\mathbf{r})$$

apply where $q(k,\omega,\mathbf{r})$ is the local velocity spectrum function, assumed to be given in the mixing-length approximation by

$$q\,(k,\omega,\mathbf{r}) = 2\left\langle u^{(0)\,2}(\mathbf{r})\right\rangle\delta\,(\omega)\,\delta\left(k-\ell_{\rm cor}^{-1}\right), \tag{19}$$

where $\ell_{\rm cor}$ is the correlation length of the fluctuations or mixing length, which is connected with the correlation time $\tau_{\rm cor}$ by $\ell_{\rm cor}/\tau_{\rm cor} \approx u_{\rm c} = \sqrt{\langle u^2\rangle}$ (*cf.* Kichatinov, 1991). Similarly, the spectrum of the magnetic background fluctuations is assumed to satisfy

$$\left\langle\hat{b}_i^{(0)}(\mathbf{z},\omega)\hat{b}_j^{(0)}\left(\mathbf{z}',\omega'\right)\right\rangle = \frac{\hat{\mathcal{B}}\,(k,\omega,\kappa)}{16\pi k^2}\delta(\omega+\omega')$$
$$\times\left(\pi_{ij}(\mathbf{k}) + \frac{1}{2k^2}(\kappa_i k_j - \kappa_j k_i)\right), \tag{20}$$

$$\left\langle b^{(0)2}\right\rangle = \int \mathcal{B}\,(k,\omega,\mathbf{r})\,\mathrm{d}k\,\mathrm{d}\omega, \tag{21}$$

with a local magnetic energy spectrum function ($\mathcal{B}(k,\omega,\mathbf{r})$) and its Fourier transform ($\hat{\mathcal{B}}(k,\omega,\kappa)$). Furthermore, we use an equipartition assumption for the local

kinetic and magnetic energy spectra, that is

$$\mathcal{B}(k, \omega, \mathbf{r}) = 2\left\langle b^{(0)\,2}(\mathbf{r})\right\rangle \delta(\omega)\, \delta\left(k - \ell_{\mathrm{cor}}^{-1}\right), \tag{22}$$

with

$$\left\langle b^{(0)\,2}(\mathbf{r})\right\rangle = \rho\mu_0 \left\langle u^{(0)\,2}(\mathbf{r})\right\rangle. \tag{23}$$

The coefficient of the α-effect is calculated as the tensorial coefficient of proportionality between the turbulent emf ($\boldsymbol{\mathcal{E}}$) and the mean magnetic field ($\langle\mathbf{B}\rangle$). The emf ($\boldsymbol{\mathcal{E}}$) can be written as the sum of a hydrodynamic and a magnetic contribution:

$$\rho\boldsymbol{\mathcal{E}} = \langle\mathbf{m}\times\mathbf{b}\rangle^{(h)} + \langle\mathbf{m}\times\mathbf{b}\rangle^{(m)}. \tag{24}$$

In Equation (24), the label $^{(h)}$ means that the corresponding part is calculated for the case of no magnetic background fluctuations, while the label $^{(m)}$ means that the external force ($\mathbf{f}$) is neglected but the electric background field (ε) drives the turbulence. That is to say, we are using a perturbation expansion with $|\langle\mathbf{B}\rangle|$ as a small parameter, taking into account only terms linear in $\langle\mathbf{B}\rangle$.

Equation (24) implies that the tensor α can also be written as the sum of a hydrodynamic part ($\alpha^{(h)}$) and a magnetic part ($\alpha^{(m)}$). These can in turn both be written as the sum of two contributions resulting from the stratification of density and turbulence intensity, respectively, so that

$$\alpha = \alpha^{(h,\rho)} + \alpha^{(h,u)} + \alpha^{(m,\rho)} + \alpha^{(m,u)}, \tag{25}$$

where the upper indices ρ and u denote contributions due to the stratification of density and turbulence intensity, respectively. For the case of rigid rotation, the hydrodynamic part of the α-effect, which corresponds to the usual kinematic contribution and is given by the first and the second summand on the right-hand side of Equation (25), was calculated using a slightly different turbulence model by Rüdiger and Kichatinov (1993).

The mean values of the fluctuating parts of the kinetic and current helicity densities are calculated according to

$$\langle h_{\mathrm{k}}\rangle = \langle\mathbf{u}\cdot(\nabla\times\mathbf{u})\rangle^{(h)}, \tag{26}$$

$$\langle h_{\mathrm{c}}\rangle = \langle\mathbf{b}\cdot(\nabla\times\mathbf{b})\rangle, \tag{27}$$

where in Equation (26) $\mathbf{u}$ is the fluctuating velocity as driven by the force $\mathbf{f}$ in the absence of magnetic fields; here and in the following h_{k} and h_{c} refer to the small-scale helicities, rather than to the sum of small-scale and large-scale ones.

3.2. Explicit expressions

For the solar dynamo, the azimuthal α-effect, *i.e.*, the component $\alpha_{\varphi\varphi}$ of the tensor α is most important. This component is responsible for the generation of the mean poloidal from the mean toroidal field and is presumably large compared to the

other components. The final expression for $\alpha_{\varphi\varphi}$, including all contribution given in Equation (25) and taking into account the effect of differential rotation for each of them, reads

$$\begin{aligned}\alpha_{\varphi\varphi} = &-\left\langle u^{(0)\,2}\right\rangle \tau_{\rm cor}\left(\cos(\theta)\Psi^{(u)}\frac{\partial}{\partial r}\log\left(\rho S\left\langle u^{(0)\,2}\right\rangle\tau_{\rm cor}\right)\right.\\ &-\frac{\partial}{\partial r}\log\left(\rho\left\langle u^{(0)\,2}\right\rangle\tau_{\rm cor}\right)\left[\Psi_{\alpha 1}\cos(\theta)\sin^2(\theta)\frac{\partial\log(\Omega)}{\partial\log(r)}\right.\\ &\left.\left.+\ \sin(\theta)\frac{\partial\log(\Omega)}{\partial\theta}(\Psi_{\alpha 2}+\cos^2(\theta)\Psi_{\alpha 1})\right]\right),\end{aligned} \tag{28}$$

where Ω^* denotes the Coriolis or inverse Rossby number, defined by $\Omega^* = 2\Omega_0\tau_{\rm cor}$ with $\Omega_0 = 2.87\times10^{-6}\,s^{-1}$ being the surface rotation rate, and $\Psi^{(u)}$, S, $\Psi_{\alpha 1}$ and $\Psi_{\alpha 2}$ are functions of Ω^* given in the Appendix.

Similarly, using Equations (26) and (27) we get for the fluctuating parts of the kinetic helicity and current helicity

$$\begin{aligned}\langle h_{\rm k}\rangle = &\left\langle u^{(0)\,2}\right\rangle\left(\cos(\theta)F_1\frac{\partial}{\partial r}\log\left(\rho\sqrt{\left\langle u^{(0)\,2}\right\rangle}\right)\right.\\ &+\Omega^*\frac{\partial}{\partial r}\log\left(\rho\left\langle u^{(0)\,2}\right\rangle\right)\left[\Psi_{h1}\cos(\theta)\sin^2(\theta)\frac{\partial\log(\Omega)}{\partial\log(r)}\right.\\ &\left.\left.+\ \sin(\theta)\frac{\partial\log(\Omega)}{\partial\theta}(\Psi_{h0}+\cos^2(\theta)\Psi_{h1})\right]\right),\end{aligned} \tag{29}$$

$$\begin{aligned}\langle h_{\rm c}\rangle = &-\sin(\theta)\frac{\Omega^*}{12}\left\langle b^{(0)\,2}\right\rangle\frac{\partial}{\partial r}\log\left(\rho\left\langle u^{(0)\,2}\right\rangle\right)\frac{\partial\log(\Omega)}{\partial\theta}\\ &+\langle B\rangle^2\left(\cos(\theta)F_2\frac{\partial}{\partial r}\log\left(\rho\sqrt{\left\langle u^{(0)\,2}\right\rangle}\right)\right.\\ &+\frac{\partial}{\partial r}\log\left(\rho\left\langle u^{(0)\,2}\right\rangle\right)\left[\Psi_{h2}\cos(\theta)\sin^2(\theta)\frac{\partial\log(\Omega)}{\partial\log(r)}\right.\\ &\left.\left.+\ \sin(\theta)\frac{\partial\log(\Omega)}{\partial\theta}(\Psi_{h3}+\cos^2(\theta)\Psi_{h2})\right]\right),\end{aligned} \tag{30}$$

where $\Psi_{h(0-3)}$ and $F_{1,2}$, are further functions of Ω^* given in the Appendix.

For a qualitative discussion of limiting cases, such as the limits of slow ($\Omega^* \ll 1$) and fast ($\Omega^* \gg 1$) rotation, and of the influence of the different contributions to the α-effect and the helicities, we refer to a companion paper (Pipin, Seehafer, and Kuzanyan, 2005). In Section 4, Equations (28) and (29) are evaluated numerically for the case of the solar convection zone using input data from a standard model of the solar interior and from helioseismic measurements.

As a theoretical quantity to be compared with the magnetic field line twist observed at the solar surface we define, in analogy to the force-free parameter $\alpha_{\rm ff}$ of the atmospheric magnetic field, a magnetic-twist parameter γ by

$$\gamma = \langle h_{\rm c} \rangle / \langle b^2 \rangle. \tag{31}$$

As is seen from Equation (30), the small-scale current helicity has two distinct contributions. One is due to the shear action of the mean velocity field $\mathbf{V}$ on the magnetic background fluctuations and is independent of the mean magnetic field ($\langle \mathbf{B} \rangle$). The other one results from the interaction of the mean magnetic field with helical velocity fluctuations (driven mechanically or magnetically) and is proportional to $\langle \mathbf{B} \rangle^2$. Then, in order to get rid of the unknown field $\langle \mathbf{B} \rangle$, the twist parameter is approximated by normalising the two contributions separately, so that

$$\gamma \approx \gamma^{(\rm shear)} + \gamma^{(\langle \mathbf{B} \rangle)}, \tag{32}$$

where $\gamma^{(\rm shear)}$ is the twist of the field generated by the action of shear on the background field $\mathbf{b}^{(0)}$, and $\gamma^{(\langle \mathbf{B} \rangle)}$ that of the field generated by the interaction of $\mathbf{u}$ with $\langle \mathbf{B} \rangle$ (which is influenced by the shear too).

4. Estimates for $\alpha_{\varphi\varphi}$, γ and $\langle h_{\rm k} \rangle$ in the Solar Convection Zone

To get estimates for $\alpha_{\varphi\varphi}$, γ and $\langle h_{\rm k} \rangle$ in the convection zone, we use radial profiles of the turbulent convective velocity ($u_{\rm c}$) and of the correlation length ($\ell_{\rm cor}$) of the turbulence derived from a standard model of the solar interior (Stix, 2002). For details of the procedure applied here, which treats the turbulence in the mixing-length approximation with the standard value 1.6 for the mixing-length parameter (α_{MLT} = ratio of correlation length to pressure scale height), we refer to Kitchatinov and Rüdiger (1999). Also used is a realistic profile $\Omega(r, \theta)$ of the solar internal rotation obtained by means of helioseismic inversions by Schou *et al.* (1998) in the form of an analytical fit given by Belvedere, Kuzanyan, and Sokoloff (2000). The profiles of the internal differential rotation rate (Ω), the Coriolis number (Ω^*), and the mean convective velocity ($u_{\rm c}$) through the convection zone are shown in Figure 2.

The convective velocity from the standard model is continued downward through the thin transition or overshoot layer between the convection zone and the rigidly rotating radiative interior by means of an analytical model of the form

$$u(r) = u_{\rm b} \left(1 - \tanh \frac{r_{\rm b} - r}{d} \right), \tag{33}$$

where $r_{\rm b}$ marks the bottom of the convection zone, $u_{\rm b}$ is the convective velocity at $r = r_{\rm b}$ and d the half width of the overshoot layer. The values used in the numerical calculations are $r_{\rm b} = 0.715 R_\odot$ and $d = 0.014 R_\odot$ and the overshooting is followed down to $0.69 R_\odot$. The Coriolis number Ω^* is fixed to its value at $r = r_{\rm b}$ throughout

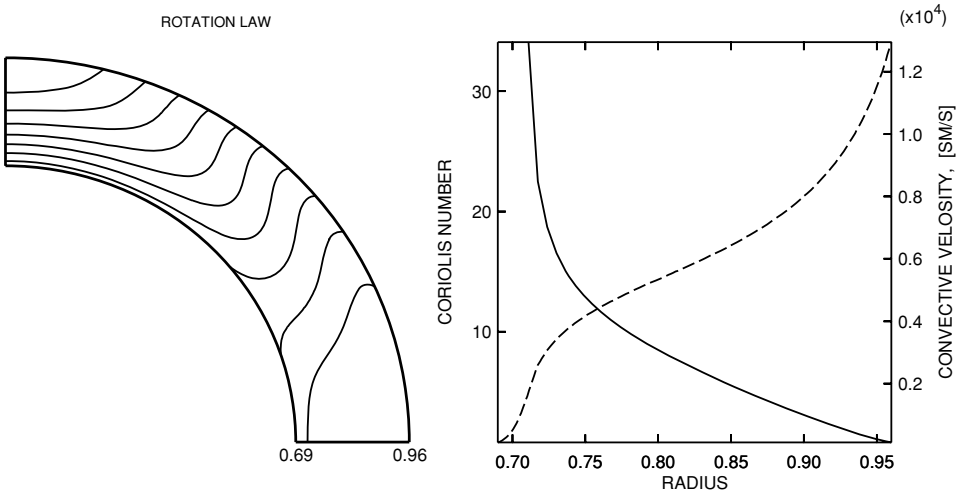

Figure 2. (*Left panel*) Contours of the rotation rate Ω in the convection zone. (*Right panel*) Radial profiles of the Coriolis number Ω^* (non-dimensional, *left scale*, *solid line*) and the convective velocity u_c (in cm s^{-1}, *right scale*, *dashed line*). The radius is given in units of $R_\odot$. Similar to Seehafer *et al.* (2003).

the layer. A similar model for the transition region has been earlier used by Rüdiger and Brandenburg (1995).

With the above profiles as input data, $\alpha_{\varphi\varphi}$, the helicities and the twist parameter γ were calculated numerically using Equations (28) – (30) and (32). Results of the calculations are given in Figures 3 – 5. Figure 3 shows, by means of greyscales and contour lines, the general distributions of $\langle h_k \rangle$, $\alpha_{\varphi\varphi}$ and γ in the solar convection zone for the northern hemisphere. The best-known observational fact here is the hemispheric sign rule for the current helicity at the surface (negative helicity in the northern and positive helicity in the southern hemisphere). Therefore the sign of the calculated quantities in the convection zone is of particular interest. It is seen in Figure 3 (upper left and bottom left) that both $\langle h_k \rangle$ and γ are negative in the upper, larger part of the convection zone, but are positive in a layer close to the bottom (the sign of γ coincides with that of the current helicity, see definition of γ by Equation (31)). In accordance with the expectation that the coefficient of the α-effect should in general be opposite in sign to both kinetic and current helicity – *cf.* Equations 2 and 5 – $\alpha_{\varphi\varphi}$ is found to be positive in the bulk of the convection zone and negative in a layer close to the bottom (Figure 3, middle left). This behaviour of $\langle h_k \rangle$, γ and $\alpha_{\varphi\varphi}$ is further illustrated in Figure 4, where radial profiles of these quantities at a latitude of 30° are shown. Altogether, these results lead us to conclude that the current helicity and the magnetic field line twist observed at the solar surface are generated in the middle or upper parts of the convection zone rather than in a layer close to the bottom where the dynamo for (at least) the toroidal solar main field is believed to operate.

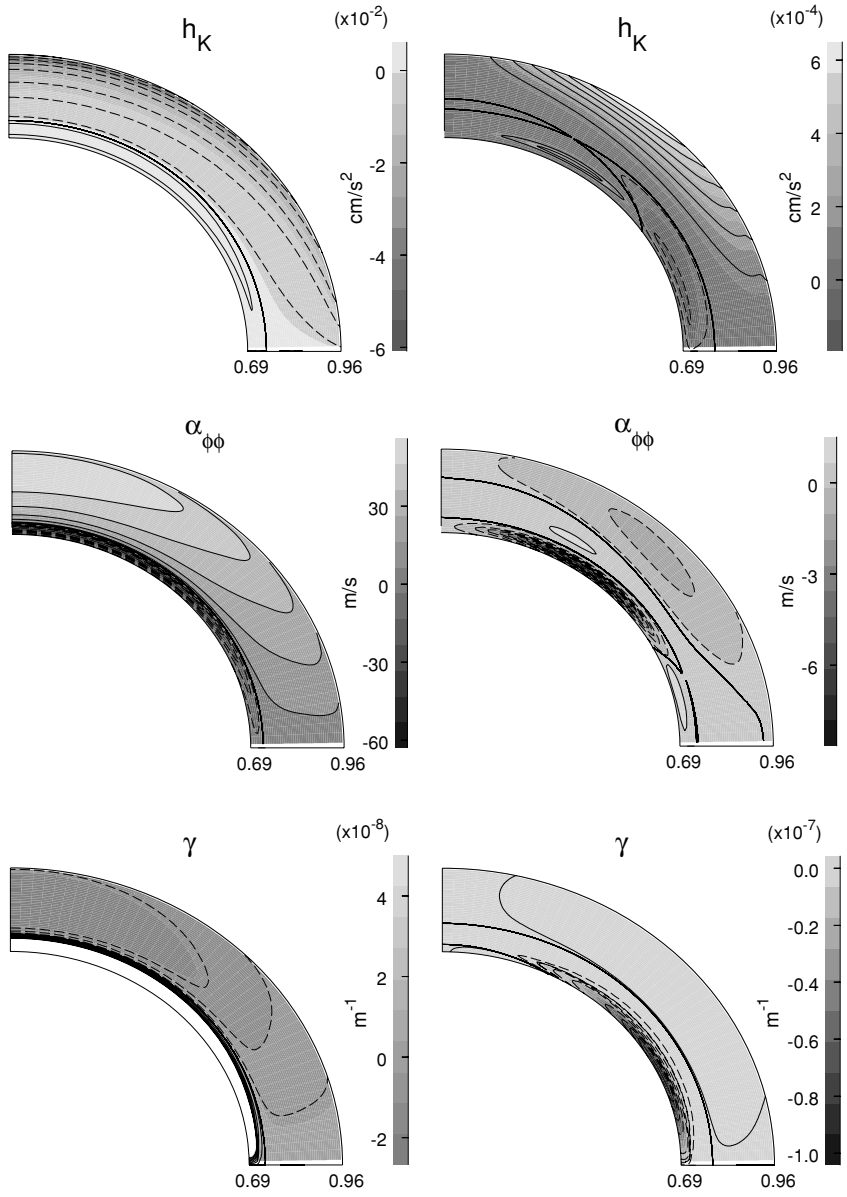

Figure 3. Computed distributions of the mean value of h_k (*upper left*), $\alpha_{\varphi\varphi}$ (*middle left*) and γ (*bottom left*) in the northern hemisphere. On the right the contributions of differential rotation to these quantities are shown. *Solid* (*dashed*) lines refer to *positive* (*negative*) values.

A typical absolute value for the observed magnetic field line twist, *i.e.*, for the factor $\alpha_{\rm ff}$, is $(1, \ldots, 1.5) \times 10^{-8}\, m^{-1}$ (see Figure 1(b) in Section 2). In the theoretical model such values of the line twist, *i.e.*, of the modulus of the factor γ (Figure 4, left panel) are obtained at about $0.8\, R_\odot$. Here we have implicitly assumed

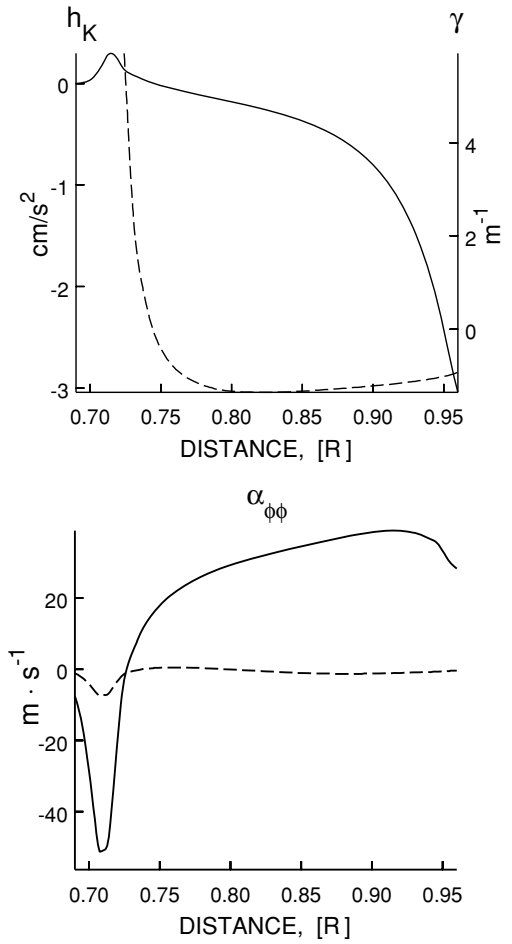

Figure 4. Radial profiles of $\langle h_k \rangle$, γ and $\alpha_{\varphi\varphi}$ at a latitude of 30°, with the radial distance given in units of $R_\odot$. (*Upper panel*) Profiles of $\langle h_k \rangle$ (*solid line*, *left scale*, in 10^{-2} sm s^{-2}), and γ (*dashed line*, *right scale*, in 10^{-8}m^{-1}). (*Lower panel*) Profile of $\alpha_{\varphi\varphi}$ (*solid line*, in m s^{-1}), with the contribution of differential rotation shown separately (*dashed line*).

that the twist (γ) of the magnetic field in the convection zone propagates upward to atmospheric levels where it is observable as the twist ($\alpha_{\rm ff}$) of the force-free magnetic field. We wish to emphasise that the physical processes by which magnetic flux generated in the convection zone is transported to the surface are poorly understood at present. Thus the direct comparison of convection-zone and atmospheric twists can only be preliminary from which, perhaps, guidance for future studies can be obtained.

From the observational data presented in Section 2, we could see that the modulus of $\alpha_{\rm ff}$ (like that of the current helicity) increases rather steeply from zero at the

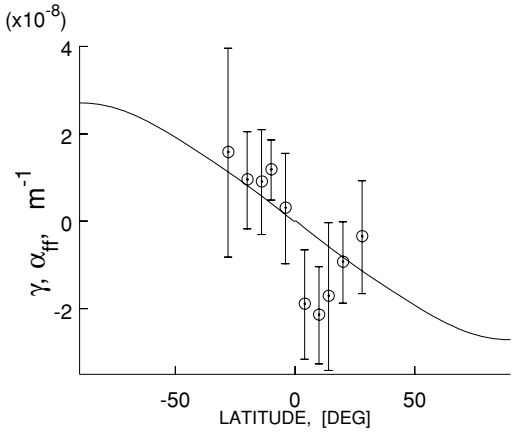

Figure 5. Calculated latitudinal profile of γ for a depth of $0.8R_\odot$. Also shown are measurements of the force-free twist factor ($\alpha_{\rm ff}$), including error bars.

equator towards higher latitudes and attains a certain saturation at about $12 - 15^\circ$. In Figure 5, the calculated latitudinal profile of γ at a depth of $0.8R_\odot$ is shown. The variable $|\gamma|$ is seen to increase more gradually and up to high latitudes. Thus we have to state that the observed latitudinal profile of the magnetic twist is not well reproduced in our model calculations.

5. Discussion

In the mean-field concept of the solar dynamo, the mean magnetic field does not reflect the magnetic fields of individual active regions. Although these fields contribute to the mean field, they are presumably mainly fluctuations. The magnetic fields observed in active regions and their helicities thus primarily give information on the fluctuating part of the magnetic field. On the basis of this assumption, we have presented a straightforward comparison of model calculations for the α-effect, helicities, and magnetic field line twist in the convection zone with magnetic field observations at atmospheric levels. The model calculations were carried out in a mixing-length approximation for the turbulence in the convection zone using a realistic profile $\Omega(r, \theta)$ of the solar internal rotation rate obtained by means of helioseismic inversions. The profiles of further quantities needed to evaluate the model, namely of the turbulent convective velocity ($u_{\rm c}$) and of the correlation length ($\ell_{\rm cor}$) of the turbulence, were derived from a standard model of the solar interior.

The magnetic field data used were photospheric vector magnetograms of 422 active regions observed with the Vector Magnetograph at Huairou Solar Observing Station in the period 1988 – 1997. From these data, averaged values of the force-free twist parameter $\alpha_{\rm ff}$ and of the current helicity $h_{\rm c}$ were calculated. This provided us with the latitudinal fine structure of these two tracers of the α-effect.

Thus, in this paper we carried out simultaneous calculations of the α-effect factor ($\alpha_{\varphi\varphi}$), the mean small-scale kinetic and current helicity densities ($\langle h_{\rm k}\rangle$ and $\langle h_{\rm c}\rangle$) and the twist factor (γ) of the small-scale magnetic field for the solar convection zone. In the model calculations, all of these quantities were found to change their sign with latitude across the equator (hemispheric rule) and with depth close to the bottom of the convection zone. Coincidence with the hemispheric sign rule for the current helicity and the magnetic field line twist observed at the surface of the Sun is obtained if these quantities are generated in the bulk of the convection zone, rather than in a layer close to the bottom. Accepting the general conviction that the large-scale toroidal field is generated by the Ω-effect close to the bottom, where the velocity shear is strong, this supports two-layer dynamo models where the Ω-effect and α-effect are operating in different layers – the Ω-effect in a thin layer at the bottom and the α-effect in the middle or upper parts of the convection zone. The α-effect could, for instance, come about by the action of helical turbulent convection on rising magnetic flux tubes, similar to the Σ-effect scenario (Longcope, Fisher, and Pevtsov, 1998; Longcope *et al.*, 1999; Longcope and Pevtsov, 2003).

Our previous observational finding was that the moduli of the average twist factor ($\alpha_{\rm ff}$) and of the current helicity density increase rather steeply from zero at the equator towards higher latitudes and attain a certain sort of saturation at about 12 – 15°. These latitudinal profiles could not be reproduced in the model calculations – in the model the increase is more gradual and continues to higher latitudes. This clearly indicates that the model needs to be developed further. For instance, the coupling between small-scale and large-scale current and magnetic helicities and the time evolution over the solar cycle, *i.e.*, the latitudinal drift of the activity belts, are still completely left out. However, whether the inclusion of these additional effects actually solves the discrepancy between theory and observations can only be answered by evaluating refined models in the future. On the other hand, the the existence of the plateau in the data still needs to be confirmed by the analysis of more additional observational material. Also observational improvements would be helpful, *e.g.*, direct or indirect information on transverse photospheric currents. This all must be left for future studies aimed at bridging the still large gap between the theory of the solar dynamo and solar magnetic field measurements.

Acknowledgements

The authors K.M.K. and V.V.P. thank RFBR for support under Grants Nos. 03-02-16384, 05-02-16090, 02-02-39027/05-02-39017, and 05-02-16326. V.V.P. furthermore acknowledges support under Grant 733.2003.2. The authors are grateful to the anonymous referee for constructive criticism and comments which helped to improve the paper.

Appendix

$$S = \Psi^{(\rho)} / \Psi^{(u)}$$

$$\Psi^{(\rho)} = \frac{1}{6\Omega^{*3}} \left(3(\Omega^{*4} - 1) \frac{\arctan \Omega^*}{\Omega^*} - (\Omega^{*2} - 3) \right)$$

$$\Psi^{(u)} = \frac{1}{12\Omega^{*3}} \left(3(\Omega^{*2} + 1)^2 \frac{\arctan \Omega^*}{\Omega^*} - (5\Omega^{*2} + 3) \right)$$

$$F_1 = \frac{1}{2\Omega^*} \left((\Omega^{*2} - 1) \frac{\arctan \Omega^*}{\Omega^*} + 1 \right)$$

$$\Psi_{\alpha 1} = \frac{1}{384\Omega^{*3}} \left(3(25\Omega^{*4} + 288\Omega^{*2} + 455) \frac{\arctan \Omega^*}{\Omega^*} - \frac{469\Omega^{*2} + 1774\Omega^{*2} + 1365}{\Omega^{*2} + 1} \right)$$

$$\Psi_{\alpha 2} = -\frac{1}{192\Omega^{*3}} \left(3(6\Omega^{*4} + 83\Omega^{*2} + 113) \frac{\arctan \Omega^*}{\Omega^*} - \frac{142\Omega^{*4} + 475\Omega^{*2} + 339}{\Omega^{*2} + 1} \right)$$

$$\Psi_{h0} = -\frac{1}{8\Omega^*} \left((\Omega^{*2} - 3) \frac{\arctan \Omega^*}{\Omega^*} + \frac{\Omega^{*2} + 3}{\Omega^{*2} + 1} \right)$$

$$\Psi_{h1} = -\frac{1}{16\Omega^*} \left((\Omega^{*2} - 1) \frac{\arctan \Omega^*}{\Omega^*} + 1 \right)$$

$$\Psi_{h2} = -\frac{1}{96\Omega^{*3}} \left(3(3\Omega^{*4} + 42\Omega^{*2} + 55) \frac{\arctan \Omega^*}{\Omega^*} - 71\Omega^{*2} - 165 \right)$$

$$\Psi_{h3} = -\frac{1}{192\Omega^{*3}} \left(-3(5\Omega^{*2} + 17)(\Omega^{*2} + 1) \frac{\arctan \Omega^*}{\Omega^*} - 49\Omega^{*2} - 51 \right)$$

$$F_2 = \frac{1}{2\Omega^{*3}} ((\Omega^{*4} - 2\Omega^{*2} - 3) \frac{\arctan \Omega^*}{\Omega^*} + (\Omega^{*2} + 3))$$

References

Abramenko, V.I., Wang, T., and Yurchishin, V.B.: 1996, *Solar Phys.* **168**, 75.
Bao, S. and Zhang, H.: 1998, *Astrophys. J.* **496**, L43.
Belvedere, G., Kuzanyan, K.M., and Sokoloff, D.: 2000, *Mon. Not. R. Astron. Soc.* **315**, 778.
Berger, M.A. and Ruzmaikin, A.A.: 2000, *J. Geophys. Res.* **105**, 10481.
Boström, R.: 1973, *Astrophys. Space Sci.* **22**, 353.

Bothmer, V. and Schwenn, R.: 1998, *Ann. Geophys.* **16**, 1.
Canfield, R.C., Hudson, H.S., and McKenzie, D.E.: 1999, *Geophys. Res. Lett.* **26**, 627.
Dasso, S., Mandrini, C.H., Démoulin, P., and Farrugia, C.J.: 2003, *J. Geophys. Res.* **108**, 1362, doi: 10.1029/2003JA009942.
Démoulin, P., Mandrini, C.H., van Driel-Gesztelyi, L., López Fuentes, M.C., and Aulanier, G.: 2002, *Solar Phys.* **207**, 87.
DeVore, C.R.: 2000, *Astrophys. J.* **539**, 944.
Ding, Y.J., Hong, Q.F., and Wang, H.Z.: 1987, *Solar Phys.* **107**, 221.
Durney, B.R. and Spruit, H.C.: 1979, *Astrophys. J.* **234**, 1067.
Duvall, Jr., T.L. and Gizon, L.: 2000, *Solar Phys.* **192**, 177.
Frisch, U., Pouquet, A., Léorat, J., and Mazure, A.: 1975, *J. Fluid Mech.* **68**, 769.
Hagino, M. and Sakurai, T.: 2004, *Publ. Astron. Soc. Japan* **56**, 831.
Hale, G.E.: 1927, *Nature* **119**, 708.
Keinigs, R.K.: 1983, *Phys. Fluids* **26**, 2558.
Kichatinov, L.L.: 1987, *Geophys. Astrophys. Fluid Dyn.* **38**, 273.
Kichatinov, L.L.: 1991, *Astron. Astrophys.* **243**, 483.
Kichatinov, L.L. and Rüdiger, G.: 1992, *Astron. Astrophys.* **260**, 494.
Kitchatinov, L.L. and Rüdiger, G.: 1999, *Astron. Astrophys.* **344**, 911.
Kleeorin, N.I. and Ruzmaikin, A.A.: 1982, *Magnetohydrodynamics* **18**, 116.
Kleeorin, N., Kuzanyan, K., Moss, D., Rogachevskii, I., Sokoloff, D., and Zhang, H.: 2003, *Astron. Astrophys.* **409**, 1097.
Krause, F. and Rädler, K.-H.: 1980, *Mean-Field Magnetohydrodynamics and Dynamo Theory*, Akademie-Verlag, Berlin.
Kuzanyan, K., Bao, S., and Zhang, H.: 2000, *Solar Phys.* **191**, 231.
Leamon, R.J., Canfield, R.C., and Pevtsov, A.A.: 2004, *J. Geophys. Res.* **109**, A05106, doi: 10.1029/2003JA010324.
Longcope, D.W. and Pevtsov, A.A.: 2003, *Adv. Space Res.* **32**, 1845.
Longcope, D.W., Fisher, G.H., and Pevtsov, A.A.: 1998, *Astrophys. J.* **507**, 417.
Longcope, D., Linton, M., Pevtsov, A., Fisher, G., and Klapper, I.: 1999, in M.R. Brown, R.C. Canfield, and A.A. Pevtsov (eds.), *Magnetic Helicity in Space and Laboratory Plasmas. Vol. 111: Geophysical Monographs*, Am. Geophys. U., Washington, DC, p. 93.
López Fuentes, M.C., Démoulin, P., Mandrini, C.H., Pevtsov, A.A., and van Driel-Gesztelyi, L.: 2003, *Astron. Astrophys.* **397**, 305.
Low, B.C.: 2001, *J. Geophys. Res.* **106**, 25141.
Martin, S.F.: 1998, in D. Webb, D. Rust, and B. Schmieder (eds.), *New Perspectives on Solar Prominences. Vol. 150: ASP Conf. Ser.*, Astronomical Society of the Pacific, San Francisco, p. 419.
Martin, S.F., Bilimoria, R., and Tracadas, P.W.: 1994, in R.J. Rutten and C.J. Schrijver (eds.), *Solar Surface Magnetism*, Kluwer, Dordrecht, p. 303.
Matthaeus, W.H., Goldstein, M.L., and Lantz, S.R.: 1986, *Phys. Fluids* **29**, 1504.
Moffatt, H.K.: 1978, *Magnetic Field Generation in Electrically Conducting Fluids*, Cambridge University Press, Cambridge, England.
Ossendrijver, M.: 2003, *Astron. Astrophys. Rev.* **11**, 287.
Parker, E.N.: 1979, *Cosmical Magnetic Fields*, Clarendon Press, Oxford.
Pevtsov, A.A.: 2002, in P.C.H. Martens and D.P. Cauffman (eds.), *Multi-Wavelength Observations of Coronal Structure and Dynamics. Vol. 13: COSPAR Colloq.*, Pergamon, Dordrecht, p. 125.
Pevtsov, A.A. and Canfield, R.C.: 1999, in M.R. Brown, R.C. Canfield, and A.A. Pevtsov (eds.), *Magnetic Helicity in Space and Laboratory Plasmas. Vol. 111: Geophysical Monographs*, Am. Geophys. U., Washington, DC, p. 103.
Pevtsov, A.A. and Latushko, S.M.: 2000, *Astrophys. J.* **528**, 999.
Pevtsov, A.A., Canfield, R.C., and Latushko, S.M.: 2001, *Astrophys. J.* **549**, L261.

Pevtsov, A.A., Canfield, R.C., and Metcalf, T.R.: 1995, *Astrophys. J.* **440**, L109.
Pipin, V.V.: 2003, *Geophys. Astrophys. Fluid Dyn.* **97**, 25.
Pipin, V.V., Seehafer, N., and Kuzanyan, K.M.: 2006, *Astron. Astrophys.* (in preparation).
Pouquet, A., Frisch, U., and Léorat, J.: 1976, *J. Fluid Mech.* **77**, 321.
Raadu, M.A.: 1972, *Solar Phys.* **22**, 443.
Rädler, K.-H. and Seehafer, N.: 1990, in H.K. Moffatt and A. Tsinober (eds.), *Topological Fluid Mechanics*, Cambridge University Press, Cambridge, England, p. 157.
Richardson, R.: 1941, *Astrophys. J.* **93**, 24.
Roberts, P.H. and Soward, A.M.: 1992, *Ann. Rev. Fluid Mech.* **24**, 459.
Rüdiger, G. and Arlt, R.: 2003, in A. Ferriz-Mas and M. Núñez (eds.), *Advances in Nonlinear Dynamos*, Taylor and Francis, London, p. 147.
Rüdiger, G. and Brandenburg, A.: 1995, *Astron. Astrophys.* **296**, 557.
Rüdiger, G. and Kichatinov, L.L.: 1993, *Astron. Astrophys.* **269**, 581.
Rüdiger, G. and Pipin, V.V.: 2000, *Astron. Astrophys.* **362**, 756.
Rüdiger, G., Brandenburg, A., and Pipin, V.V.: 1999, *Astron. Nachr.* **320**, 135.
Rüdiger, G., Pipin, V.V., and Belvedere, G.: 2001, *Solar Phys.* **198**, 241.
Rust, D.M.: 1994, *Geophys. Res. Lett.* **21**, 241.
Rust, D.M.: 2001, *J. Geophys. Res.* **106**, 25075.
Rust, D.M. and Kumar, A.: 1994, *Solar Phys.* **155**, 69.
Rust, D.M. and Kumar, A.: 1996, *Astrophys. J.* **464**, L199.
Ruzmaikin, A.A., Martin, S., and Hu, Q.: 2003, *J. Geophys. Res.* **108**, 1096, doi: 10.1029/2002JA009588.
Schou, J., Antia, H.M., Basu, S., Bogart, R.S., Bush, R.I., Chitre, S.M., Christensen-Dalsgaard, J., Di Mauro, M.P., Dziembowski, W.A., Eff-Darwich, A., Gough, D.O., Haber, D.A., Hoeksema, J.T., Howe, R., Korzennik, S.G., Kosovichev, A.G., Larsen, R.M., Pijpers, F.P., Scherrer, P.H., Sekii, T., Tarbell, T.D., Title, A.M., Thompson, M.J., and Toomre, J.: 1998, *Astrophys. J.* **505**, 390.
Seehafer, N.: 1990, *Solar Phys.* **125**, 219.
Seehafer, N.: 1994, *Europhys. Lett.* **27**, 353.
Seehafer, N.: 1996, *Phys. Rev. E* **53**, 1283.
Seehafer, N., Gellert, M., Kuzanyan, K.M., and Pipin, V.V.: 2003, *Adv. Space Res.* **32**, 1819.
Steenbeck, M., Krause, F., and Rädler, K.-H.: 1966, *Z. Naturforsch.* **21a**, 369.
Stix, M.: 2002, *The Sun. An Introduction*, 2nd edn., Springer, Berlin.
van Ballegooijen, A.A. and Martens, P.C.H.: 1990, *Astrophys. J.* **361**, 283.
van Ballegooijen, A.A., Cartledge, N.P., and Priest, E.R.: 1998, *Astrophys. J.* **501**, 866.
Zeldovich, Y., Ruzmaikin, A.A., and Sokoloff, D.D.: 1983, *Magnetic Fields in Astrophysics*, Gordon and Breach, New York.
Zhang, H. and Bao, S.: 1998, *Astron. Astrophys.* **339**, 880.
Zhang, H.Q., Bao, S.D., and Kuzanyan, K.M.: 2002, *Astron. Rep.* **46**, 424.
Zirker, J.B., Martin, S.F., Harvey, K., and Gaizauskas, V.: 1997, *Solar Phys.* **175**, 27.